RAPID COMMUNICATIONS

PHYSICAL REVIEW D VOLUME 47, NUMBER 11 1 JUNE 1993

Calculated electron fluxes at airplane altitudes

R. K. Schaefer, T. K. Gaisser, and T. S. Stanev
Bartol Research Institute, University of Delaware, Newark, Delaware 19716
(Received 22 February 1993)

A precision measurement of atmospheric electron fluxes has been performed on a Japanese commercial airliner (Enomoto *et al.*). The bulk of these electrons are produced in pairs from the γ rays emitted when π^0's decay, which in turn have been produced in cosmic-ray–air-nucleus collisions. These electron fluxes can be used to test elements of our atmospheric neutrino flux calculation, i.e., the assumed primary spectrum and the Monte Carlo shower code. Here we have modified the Monte Carlo program which had previously been used to calculate the fluxes of atmospheric neutrinos by combining it with the program GEANT to compute the electromagnetic part of the shower. This hybrid program now keeps track of the electrons produced in cosmic-ray showers as a function of energy and atmospheric depth. We compare our calculated integral fluxes above the experimental threshold energies 1, 2, and 4 GeV for a variety of atmospheric depths and cutoff rigidities. Our results are in good agreement ($\sim$ a few %) with the data, but we found we needed to boost the normalization of the primary flux by 12% over the value we had previously used to calculate the atmospheric neutrino flux.

PACS number(s): 96.40De, 95.85Ry, 96.40Pq

I. INTRODUCTION

The production of secondary electrons in the atmosphere from primary cosmic rays is a well known phenomenon and a detailed formalism for calculating these effects has existed for a long time. Most measurements of electron fluxes have been carried out with balloons which spend most of their time near the top of the atmosphere. Thus, most balloon measurements reflect cosmic rays which have penetrated $\sim 2-50$ g/cm^2 of atmosphere. Larger depths are not well sampled by balloons. To reach the altitudes of commercial jet aircraft, $\sim 9-12$ km, a cosmic ray shower has to penetrate $\gtrsim 200$ g/cm^2 of (vertical) material. Since this corresponds to about six electron radiation lengths, there are virtually no primary cosmic ray electrons which can penetrate to this depth. The bulk of the atmospheric electrons detected in an airplane would then be secondaries generated in showers from primary cosmic ray nucleons. As such, these electrons offer us a probe of the primary cosmic ray spectrum, and high precision measurements could potentially pin down the proper normalization of the high energy cosmic ray flux, which is uncertain (see, e.g., Ref. [1]) by about $\pm 20\%$.

In fact this uncertainty in the normalization of the high energy cosmic ray spectrum affects all calculations of cosmic ray progeny, including γ rays, antiprotons, positrons, and atmospheric neutrinos. For example, in the recent measurements of the atmospheric neutrinos, one does not know whether the detectors are seeing too few muon neutrinos or too many electron neutrinos because the expected rate depends directly on how the calculation is normalized [2].

Early treatments of electron production (see Ref. [3]) consisted of integrating a set of coupled atmospheric cascade equations. However, recent calculations of the atmospheric neutrino fluxes have been done using a detailed Monte Carlo program for cosmic ray air showers developed over a period of time. It is therefore useful, convenient, and relevant that we use this same program to calculate the electron fluxes expected in an airplane experiment. We have two main objectives in doing the calculation this way: (1) We hope to test the accuracy of the Monte Carlo program, and (2) we hope to fix the normalization of the primary nucleon energy spectrum. The results are also relevant to the calibration of balloon-borne electron spectrometers. These must measure the electron flux as the balloon rises in order to subtract the secondary component at float altitude. A precise calculation of flux versus altitude is helpful in making this subtraction. In the next section we describe how we performed the calculation, and then we will discuss our results and implications.

II. CALCULATIONS

The primary goal of our computation is to compare the fluxes measured in the Enomoto *et al.* (Ref. [4]) experiment. This procedure is quite similar to one we did for the atmospheric neutrino flux [5, 6]. We will therefore only briefly summarize the relevant parts of the calculation.

We begin by simulating cascades initiated by a primary particle of fixed energy. (An incoming nucleus of mass A is treated as A independent incident nucleons—an approximation which has been shown to correctly reproduce the uncorrelated atmospheric average fluxes of particles [7].) The primary nucleon collides with an air nucleus producing a fast fragment nucleon and many mesons, of which some decay and some interact again. All π^0 mesons produced along the shower

 ©1993 The American Physical Society

core decay essentially immediately into a pair of photons which then subsequently produce negatron-positron pairs. Occasionally other mesons will decay directly to an electron (e.g., $K_L^0 \rightarrow \pi^{\pm} e^{\mp} \nu$ or $K^+ \rightarrow \pi^0 e^+ \nu_e$). As these electrons propagate in the atmosphere, they can emit bremsstrahlung photons which later produce more negatron-positron pairs. Bremsstrahlung is the main source of energy loss for electrons in this energy range, and the calculated flux of electrons at a given depth is quite sensitive to the accuracy of the description of the bremsstrahlung process. In order to treat all electromagnetic effects (including bremstrahlung) to a high degree of accuracy we have used the program GEANT, a standard code used by high energy particle physics experimenters for calculating the particle showers that happen inside their detectors.

GEANT incorporates many electromagnetic effects which are not very important at GeV energies, but can affect the results at the few percent level. We are striving for high precision, so we used GEANT to calculate the following effects as well as the bremsstrahlung: ionization energy losses in air, Compton scattering of atomic electrons, δ ray production, and multiple scattering. GEANT does its simulations using constant density slabs of material, unlike our hadronic code which uses a continuously varying air density. The electromagnetic processes are not sensitive to the depth-altitude relationship, but the hadronic processes are (especially to the competition between decay and interaction for charged pions and kaons). Thus we achieved the following synthesis: first, we simulate the hadronic portion of the shower in a realistic atmospheric model, keeping track of the depths and energies of all of the produced photons (and electrons from direct meson decays). At each primary energy, we simulate as many showers as it takes to accumulate $> 50\,000$ particles (mostly photons with a few direct $e^{\pm}$) with energies greater than 1 GeV at altitudes above the minimum for which the Enomoto *et al.*, [4] data were taken. Then we input these photons (and electrons) into the GEANT program which uses a constant density ($\rho_{\rm air} = 1.19 \times 10^{-4}$ g/cm^3) slab of air. We then record the number of electrons which pass 20 evenly spaced depth flags between 205 and 300 g/cm^2. We repeat this process for 22 separate (roughly logarithmically spaced) primary energies for each of the three electron threshold energies 1, 2, and 4 GeV. We estimate the statistical uncertainty in our Monte Carlo program contributes $\leq 1\%$ uncertainty to the final electron fluxes.

The yields per incident primary are then multiplied by the differential primary proton spectrum to get the electron yield per primary energy interval. The primary proton spectrum used here has the same shape as that used in Ref. [6], but with a 12% higher normalization. Multiplying this quantity by the energy gives the electron yield per *logarithmic* energy interval which is plotted in Fig. 1 at a typical airplane depth (250 g/cm^2) for each of the electron energy thresholds 1, 2, and 4 GeV. One can see that the electron flux drops sharply with energy and that the average primary energy which contributes these electrons rises proportionately with the threshold energy. The primaries responsible for the electrons in these measurements are of somewhat higher energy than those responsible for the atmospheric neutrinos measured at IMB [8] and Kamiokande [9]. For example, the median primary energy for progenitors of GeV neutrinos is approximately 20 GeV/nucleon, as compared to 50 GeV/nucleon for GeV electrons. The difference is a consequence of the electromagnetic cascading process.

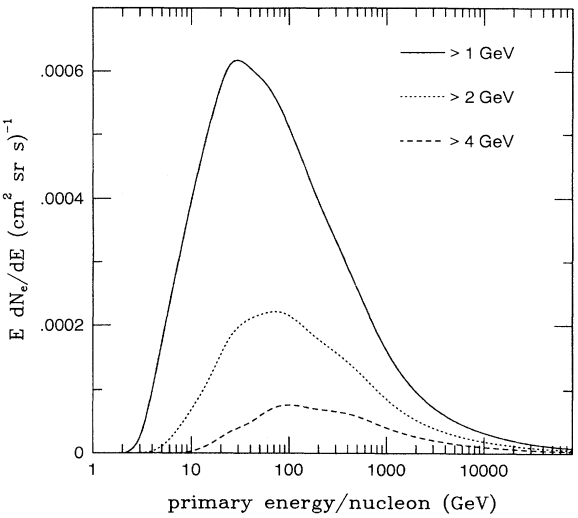

FIG. 1. Differential electron flux. The number of electrons (cm^2 s sr)$^{-1}$ per logarithmic energy interval as a function of total energy per nucleon. Note the increase in median primary energy and decrease in flux as the we increase the detector threshold energy.

To first approximation, the total electron number which would be measured at 250 g/cm^2 is just the area under the curve in Fig. 1. However, in contrast to the typical balloon experiment, the airplane experiment measured fluxes in locations where the geomagnetic primary cutoff energies are quite high (rigidities in the range 4.8–16.2 GV) and at a variety of atmospheric depths. These effects must be treated accurately. The cutoff rigidities were handled as follows. For protons, the cutoff rigidities are converted to energies, and the integration of the primary spectrum is cut off abruptly at this energy. For primary nuclei, the cut off energy per nucleon will be different (roughly a factor of 2 lower than for protons) so we include the primary nuclei separately.

The detector has an acceptance of 15° from vertical. To simulate particles which are incident to the atmosphere at an angle $\theta_{\rm incident}$ from vertical, one must scale all of the depths by a factor $1/\cos(\theta_{\rm incident})$. We have explicitly done an integration over the solid angle contained in a 15° cone in a few test cases and find the results are indistinguishable from simply scaling all of the depths to the average angle, 10.6°, and performing no additional averaging. Since $1/\cos(10.6°) = 1.02$, the slant depth is 2% larger than vertical.

Finally, we have considered secondary electrons generated from primary *electrons*. These were not included in the treatment of Ref. [3]. The primary electrons have lost enough energy via bremsstrahlung that they do not themselves contribute to the flux at airplane altitudes.

However, the bremstrahlung photons these primary electrons emit can also produce negatron-positron pairs after penetrating a bit deeper than the primary electrons. We have used the Monte Carlo program GEANT with primary electrons to simulate the electromagnetic cascades generated by primary electrons. For purposes of including electronic progenitor electrons in our airplane flux calculation, we assume that the primary electrons, although of opposite charge sign, will have the same cutoff rigidity as the protons. This approximation is adequate because cascading ensures that most of the contribution to electrons > 1 GeV at ≥ 200 g/cm^2 comes from primary electrons above the geomagnetic cutoff. For the primary electron spectrum we use the spectrum from the 1990 flight of the LEE (Low Energy Electron) balloon experiment (Ref. [10]), although using a different spectrum (1987 LEE flight) gave results indistinguishable from those presented here. When we include these secondary calculations into our results the fluxes increase by about 3% for > 1 GeV electrons and somewhat less for higher threshold energies.

The total calculation can be represented by the formula

$$N_e(> E_{\rm thr}, d_{\rm atm}, R_c) = \sum_{i=1}^{3} \int_{E_i(R_c)}^{\infty} dE \frac{dN_i}{dE} Y_i(E, E_{\rm thr}, 1.02 d_{\rm atm}) \tag{2.1}$$

Here N_e is the predicted integral electron flux above threshold energy $E_{\rm thr}$, vertical atmospheric depth $d_{\rm atm}$, and cutoff rigidity R_c. We have to sum over the different types of primaries: protons, electrons, and nuclei [which have a different cutoff energy than protons, hence the lower limit on the integral $E_i(R_c)$ depends on primary type]. The Y_i are the electron yields per incident primary of energy E and type i at a depth $d_{\rm atm}$ and electron threshold energy $E_{\rm thr}$. The 1.02 factor multiplying $d_{\rm atm}$ in the yield is to account for the fact that the average primary is incident at an angle of 10.6° as described above.

The results of these calculations are shown by the triangles in Figs. 2, 3, and 4 for energy thresholds of 1, 2, and 4 GeV, respectively. The measurements and error bars of Enomoto *et al.*, [4] are presented for comparison. These figures correspond directly to Fig. 5 of Enomoto *et al.*, but we have placed the data from both the Guam-Sydney and the Sidney-Guam flights on the same graph. Thus the data seemingly taken at nearby latitudes can in fact have been taken at quite different altitudes and cutoff rigidities. We also note here that the Enomoto *et al.* error bars are a quadrature sum of 3% statistical and 5% systematic errors.

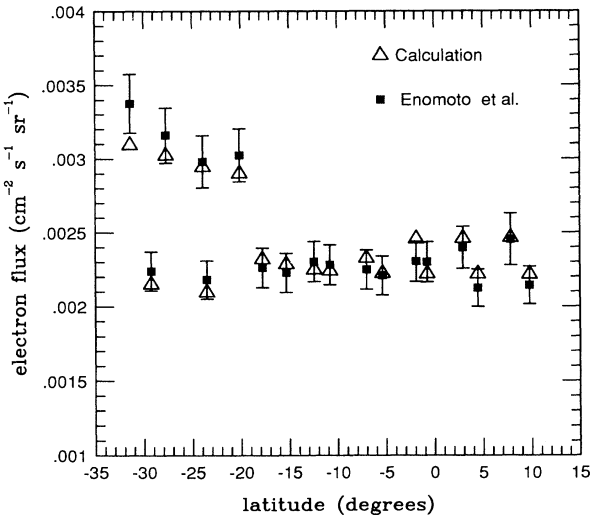

FIG. 2. Integral flux at > 1 GeV. The electron flux (cm^2 s sr)$^{-1}$ predictions for the cutoff rigidities and atmospheric depths given in Enomoto *et al.* [4]. We have plotted both the Guam-Sydney and the return flight together here as a function of the terrestrial latitude of the observation. The apparent jitter in the fluxes is due to the fact that observations at neighboring latitudes can correspond to data taken at quite different altitudes and cutoff rigidities

III. DISCUSSION AND IMPLICATIONS

Inspection of Figs. 2, 3, and 4 reveals that our calculation agrees well with the experimental results. In the plots the triangles represent our calculations and the filled boxes (with 1σ error bars) are the measurements of Enomoto *et al.* [4]. The points are taken at a variety of atmospheric depths and cutoff rigidities as the aircraft flew from high to low (terrestrial) latitude and back. We have chosen to plot the data as a function of latitude because this keeps the data points clearly separated. However, this choice of plotting does not adequately reflect the fact that points of similar latitudes can correspond to data taken at quite different altitudes

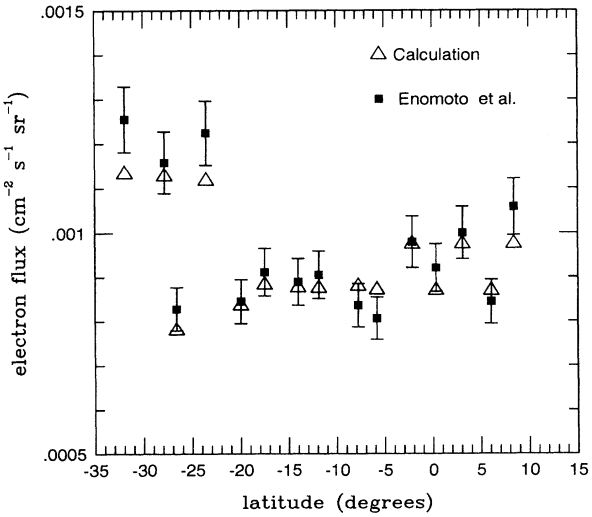

FIG. 3. Integral flux at > 2 GeV. Similar to Fig. 2, but for the electron detector threshold energy of 2 GeV.

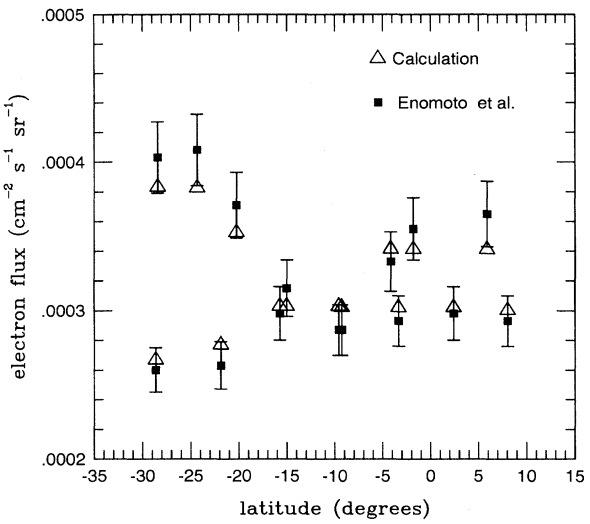

FIG. 4. Integral flux at > 4 GeV. Similar to Fig. 2, but for the electron detector threshold energy of 4 GeV.

and cutoff rigidities, which have been incorporated explicitly into the calculated fluxes. (For the altitudes and cutoff rigidities associated with observations at each latitude point, see Tables III, IV, and V in Enomoto *et al.* [1]). The data tend to be clumped around several depths and cutoff rigidities. The value of the flux is most sensitive to atmospheric depth and the highest intensities are recorded at depths of about 220 g/cm^2. The dependence of intensity on cutoff rigidity is less sensitive, although still noticeable. We can see that the general trends with depth and geomagnetic cutoff are quite well represented to get such good agreement.

From Fig. 2, we can see the > 1 GeV electron results are in remarkably good agreement with the predictions. Only 2 out of the 18 predictions are not within the $\pm 1\sigma$ error bars of the measurements, indicating perhaps that the experimental errors are slightly overestimated. Similarly the agreement in Figs. 3 and 4 is also better than would be expected from the size of the errors. For the > 2 GeV electron measurements, 4 out of the 15 points are not within $\pm 1\sigma$, while for the > 4 GeV there are only 2 out of 15 outlying points. A change of the primary flux normalization by just a few percent ruins this close agreement.

This calculation shows that our Monte Carlo program for simulating hadronic cosmic ray showers seems to work quite well. The only feature of our calculation which we could consider improving is the slight systematic underprediction of the highest altitude flux. (These points are found at the upper left corner of all of the figures.) Coincidently, these highest altitude points are also those at the lowest rigidity cutoff. If this happened only with the > 1 GeV electrons one might believe this could be caused by solar modulation of the lower energy flux. However, this underprediction shows up in the > 2 and > 4 GeV electrons as well. A check of the differential fluxes (Fig. 1) shows that almost none of the > 4 GeV electrons come from primaries which are even close to the geomagnetic cutoff energies. Thus, there may be a slight problem in that the showers do not develop high enough in the atmosphere. This discrepancy is at a level of 5%.

We have not included the contribution from "knock-on" electrons. The main source of knock-on electrons at depths > 100 g/cm^2 is collisions of muons with air atoms (see Ref. [3]). Using the formula in Daniel and Stephens [3] for producing knock-on electrons and the measured muon flux at 9 km [11] we estimate that knock-on electrons could contribute no more than 1% of the electron flux.

The excellent fit to the data requires that the normalization of the primary flux be fixed to within a few percent. Similarly, changing the spectral exponent of the primary flux will destroy the agreement of the > 4 GeV electron data relative to the > 1 GeV data. Thus the primary spectrum used in [6] for the calculation of the neutrino flux seems to have the correct shape, but the normalization should be raised by 12%. If this raised normalization extends to the lower energy part of the primary spectrum, this would imply that the corresponding neutrino fluxes should also be scaled up by 12%. We note, however, that there are systematic experimental errors which could affect this conclusion. Energy-dependent uncertainties exist in modeling the acceptance and particle energy identification [12]. Since these errors are of order 5%, the integral fluxes could change at worst by as much as $(1.05)^{1.7} = 1.09\%$ or 9%. To be very conservative we could therefore say that the electron measurements imply a normalization boost of 12 ± 9 %. We are currently investigating other indirect checks (e.g., atmospheric μ fluxes) to test the consistency of raising the normalization. We note that these electron fluxes imply tighter constraints on the primary spectrum than are currently allowed by direct measurements of the primary spectrum ($\sim \pm 20\%$).

IV. CONCLUSIONS

We have performed a Monte Carlo calculation of the atmospheric electron flux at the depths and cutoff rigidities of the Enomoto *et al.* airplane experiment. We predict integral fluxes which show excellent agreement with the > 1, > 2, and > 4 GeV electrons. The predictions generally follow the depth and cutoff rigidity trends seen in the data. The agreement is so good that it suggests that the experimental errors have been estimated very conservatively. This analysis suggests three things: (1) The hadronic Monte Carlo code used for calculating atmospheric neutrino fluxes seems to work well for another species of atmospheric secondaries, namely electrons, (2) the shape of the primary spectrum from Ref. [6] gives the correct energy spectrum of electrons from 1 GeV to 4 GeV, and (3) the normalization of the primary cosmic ray spectrum is somewhat higher than that used by Ref. [6].

ACKNOWLEDGMENTS

We thank R. Enomoto, P. Evenson, M. Honda, and T. Kifune for helpful discussions. We would also like to thank J. Petrakis for invaluable help in using GEANT. This work was supported in part by NASA Grant No. NAGW-1644.

[1] T. K. Gaisser and R. K. Schaefer, Astrophys. J. **394**, 174 (1992).
[2] E. W. Beier *et al.*, Phys. Lett. B **283**, 446 (1992).
[3] R. R. Daniel and S. A. Stephens, Rev. Geophys. Space Phys. **12**, 233 (1974).
[4] R. Enomoto *et al.*, Phys. Rev. D **44**, 3419 (1991).
[5] G. Barr, T. K. Gaisser, and T. Stanev, Phys. Rev. D **39**, 3532 (1989).
[6] T. K. Gaisser, T. Stanev, and G. Barr, Phys. Rev. D **38**, 85 (1988).
[7] J. Engel, T. K. Gaisser, P. Lipari, and T. Stanev, Phys. Rev. D **46**, 5013 (1992).
[8] D. Casper *et al.*, Phys. Rev. Lett. **66**, 2561 (1991); R. Becker-Szendy *et al.*, Phys. Rev. D **46**, 3720 (1992).
[9] K. S. Hirata *et al.*, Phys. Lett. B **205**, 416 (1988); **280**, 146 (1992).
[10] P. Evenson (private communication). For information see P. Evenson, E. B. Tuska, J. Esposito, and P. Meyer, in *Proceedings of the 22nd International Cosmic Ray Conference*, Dublin, Ireland, 1991, edited by M. Cawley *et al.* (Dublin Institute for Advanced Research, Dublin, 1992), paper SH 6.4.3.
[11] L.T. Baradzei *et al.*, Zh. Eksp. Teor. Fiz. **36**, 1617 (1959) [Sov. Phys. JETP **9**, 1151 (1959)].
[12] R. Enomoto (private communication).